Testing the littlest Higgs model with *T* parity in bottom quark pair production at high energy photon colliders

Jinshu Huang[*]

College of Physics & Information Engineering, Henan Normal University, Xinxiang 453007, People's Republic of China;
College of Physics & Electric Engineering, Nanyang Normal University, Nanyang 473061, People's Republic of China;
and Kavli Institute for Theoretical Physics China, Chinese Academy of Science, Beijing 100190, People's Republic of China

Gongru Lu[†] and Xuelei Wang[‡]

College of Physics & Information Engineering, Henan Normal University, Xinxiang 453007, People's Republic of China
and Kavli Institute for Theoretical Physics China, Chinese Academy of Science, Beijing 100190, People's Republic of China

We have calculated the cross section of the process $e^+e^- \to \gamma\gamma \to b\bar{b}$ in the littlest Higgs model with *T* parity (LHT). We find that, for the favorable parameters, the total cross section $\sigma(e^+e^- \to \gamma\gamma \to b\bar{b})$ is sensitive to the breaking scale f, mixing parameter x_L, the masses of the mirror quarks m_{Hi}, and the relative correction of the LHT model is a few percent to dozens of percent. The cross section is significantly larger than the corresponding results in the standard model and in the other typical new physics models. Therefore the prediction in the LHT model is quite different from the predictions in other new physics models and such a process is really interesting in searching for the signs of the LHT model.

I. INTRODUCTION

The electroweak symmetry breaking mechanism remains an open question in spite of the success of the standard model (SM) compared with the precision measurement data. The collisions of high energy photons produced at the linear collider provide a comprehensive laboratory for testing the SM and probing new physics beyond the SM [1]. With the advent of the new collider technique, the high energy and high intensity photon beams can be obtained by using Compton laser photons scattering off the colliding electron and positron beams [2], and a large number of heavy quark pairs can be produced by this method. The photon energy spectrums show that there are many relatively soft photons, and the production of heavy top quark will be suppressed owing to the reduction of collision energies. However, no such suppression affects the relatively light bottom quark [3]. Therefore it is worth investigating the production of the bottom quark pairs in the photon-photon collisions.

In the SM, this process has been calculated and the QCD threshold effects of the process have been also examined [4]. Reference [5] presents a study of the Yukawa corrections to this process in both the general two Higgs doublet model (2HDM) and the minimal supersymmetric standard model (MSSM), which arise from the virtual effects of the charged Higgs and charged Goldstone bosons, and show that the relative correction to the total cross section of the processes $e^+e^- \to \gamma\gamma \to b\bar{b}$ is less than 0.1% for the favorable parameter values. In Ref. [6], the authors have calculated the Yukawa correction to the cross section of

$\gamma\gamma \to b\bar{b}$ induced by the pseudo-Goldstone bosons and the new gauge bosons in the topcolor assisted technicolor (TC2) model, and pointed out that the relative correction is negative and not more than 10%. In this paper, we will study the contribution of the littlest Higgs model with *T* parity (LHT) to this process.

As we know, the fancy idea of little Higgs [7] tries to provide an elegant solution to the hierarchy problem by regarding the Higgs boson as a pseudo-Goldstone boson, whose mass is protected by an approximate global symmetry, and the quadratic divergence cancellation is due to the contributions from new particles with the same spin as the SM particles. The littlest Higgs model [8] is a cute economical implementation of the little Higgs idea, but is found to be subject to the strong constraints from electroweak precision tests [9], which would require raising the mass scale of the new particles to far above TeV scale and thus reintroduce the fine-tuning in the Higgs potential [10]. To tackle this problem, a discrete symmetry called *T* parity is proposed [11], which forbids the tree-level contributions from the heavy gauge bosons to the observables involving only the SM particles as external states. Therefore we will investigate the process $\gamma\gamma \to b\bar{b}$ in this model.

This paper is organized as follows. In Sec. II, we present a brief review of the LHT model. Section III is devoted to our analytical results of the cross section of $e^+e^- \to \gamma\gamma \to b\bar{b}$ in terms of the well-known standard notation of one-loop Feynman integrals. The numerical results and conclusions are included in Sec. IV.

II. A BRIEF REVIEW OF THE LHT MODEL

The LHT model [11–13] is based on a nonlinear sigma model describing the spontaneous breaking of a global $SU(5)$ down to a global $SO(5)$ at the scale $f \sim O(\text{TeV})$.

[*]jshuang@vip.sina.com
[†]lugongru@sina.com
[‡]wangxuelei@sina.com

From the $SU(5)/SO(5)$ breaking, there arise 14 Nambu-Goldstone bosons which are described by the ''pion'' matrix Π, given explicitly by

$$
\Pi = \begin{pmatrix}
-\frac{\omega^0}{2} - \frac{\eta}{\sqrt{20}} & -\frac{\omega^+}{\sqrt{2}} & -i\frac{\pi^+}{\sqrt{2}} & -i\phi^{++} & -i\frac{\phi^+}{\sqrt{2}} \\
-\frac{\omega^-}{\sqrt{2}} & \frac{\omega^0}{2} - \frac{\eta}{\sqrt{20}} & \frac{v+h+i\pi^0}{2} & -i\frac{\phi^+}{\sqrt{2}} & \frac{-i\phi^0+\phi^P}{\sqrt{2}} \\
i\frac{\pi^-}{\sqrt{2}} & \frac{v+h-i\pi^0}{2} & \sqrt{4/5}\,\eta & -i\frac{\pi^+}{\sqrt{2}} & \frac{v+h+i\pi^0}{2} \\
i\phi^{--} & i\frac{\phi^-}{\sqrt{2}} & i\frac{\pi^-}{\sqrt{2}} & -\frac{\omega^0}{2} - \frac{\eta}{\sqrt{20}} & -\frac{\omega^-}{\sqrt{2}} \\
i\frac{\phi^-}{\sqrt{2}} & \frac{i\phi^0+\phi^P}{\sqrt{2}} & \frac{v+h-i\pi^0}{2} & -\frac{\omega^+}{\sqrt{2}} & \frac{\omega^0}{2} - \frac{\eta}{\sqrt{20}}
\end{pmatrix}. \tag{1}
$$

Under T parity, the SM Higgs doublet

$$
H = \begin{pmatrix} -i\frac{\pi^+}{\sqrt{2}} \\ \frac{v+h+i\pi^0}{2} \end{pmatrix}, \tag{2}
$$

is T even, while the other fields including a physical scalar triplet

$$
\Phi = \begin{pmatrix} -i\phi^{++} & -i\frac{\phi^+}{\sqrt{2}} \\ -i\frac{\phi^+}{\sqrt{2}} & \frac{-i\phi^0+\phi^P}{\sqrt{2}} \end{pmatrix}, \tag{3}
$$

and heavy Goldstone bosons $\omega^\pm$, ω^0, η are T odd.

A subgroup $[SU(2) \times U(1)]_1 \times [SU(2) \times U(1)]_2$ of the $SU(5)$ is gauged, and it is broken into the SM electroweak symmetry $SU(2)_L \times U(1)_Y$ at the scale f. The Goldstone bosons ω^0, $\omega^\pm$, and η are, respectively, eaten by the new T-odd gauge bosons Z_H, W_H, and A_H, which obtain masses at the order of $O(v^2/f^2)$

$$
M_{W_H} = M_{Z_H} = fg\left(1 - \frac{v^2}{8f^2}\right),
$$
$$
M_{A_H} = \frac{fg'}{\sqrt{5}}\left(1 - \frac{5v^2}{8f^2}\right), \tag{4}
$$

with g and g' being the SM $SU(2)$ and $U(1)$ gauge couplings, respectively.

The masses of the SM T-even, Z boson and W boson are generated through eating the Goldstone bosons π^0 and $\pi^\pm$. They are given by

$$
M_{W_L} = \frac{gv}{2}\left(1 - \frac{v^2}{12f^2}\right), \qquad M_{Z_L} = \frac{gv}{2\cos\theta_W}\left(1 - \frac{v^2}{12f^2}\right). \tag{5}
$$

The photon A_L is also T even and massless.

In order to cancel the quadratic divergence of the Higgs mass coming from top loops, an additional T-even quark T_+, as a heavy partner of top quark, is introduced. The implementation of T parity then requires also a T-odd

partner T_-. To leading order, their masses are given by

$$
m_{T_+} = \frac{f}{v}\frac{m_t}{\sqrt{x_L(1-x_L)}}\left[1 + \frac{v^2}{f^2}\left(\frac{1}{3} - x_L(1-x_L)\right)\right],
$$
$$
m_{T_-} = \frac{f}{v}\frac{m_t}{\sqrt{x_L}}\left[1 + \frac{v^2}{f^2}\left(\frac{1}{3} - \frac{1}{2}x_L(1-x_L)\right)\right], \tag{6}
$$

where $x_L = \lambda_1^2/(\lambda_1^2 + \lambda_2^2)$ is the mixing parameter between the SM top quark and its heavy partner T_+ quark, in which λ_1 and λ_2 are the Yuwaka coupling constants in the Lagrangian of the top quark sector. Furthermore, for each SM quark (lepton), a copy of mirror quark (lepton) with T-odd quantum number is added in order to preserve the T parity. We denote them by u_H^i, d_H^i, ν_H^i, l_H^i, where $i = 1, 2, 3$ are the generation index. In $O(v^2/f^2)$, the masses of u_H^i and d_H^i satisfy

$$
m_{Hi}^u = \sqrt{2}\kappa_i f\left(1 - \frac{v^2}{8f^2}\right) \equiv m_{Hi}\left(1 - \frac{v^2}{8f^2}\right),
$$
$$
m_{Hi}^d = \sqrt{2}\kappa_i f \equiv m_{Hi}. \tag{7}
$$

where κ_i are the diagonalized Yukawa couplings of the mirror fermions.

The mirror fermions induce a new flavor structure and there are four Cabibbo-Kobayashi-Maskawa–like unitary mixing matrices in the mirror fermion sector: V_{Hu}, V_{Hd}, V_{Hl}, and $V_{H\nu}$. These mirror mixing matrices are involved in the charged-current, flavor-changing interactions between the SM fermions and the T-odd mirror fermions which are mediated by the T-odd heavy gauge bosons or the Goldstone bosons. V_{Hu} and V_{Hd} satisfy the relation

$$
V_{Hu}^\dagger V_{Hd} = V_{CKM}. \tag{8}
$$

Following the Refs. [12,13], V_{Hd} is parametrized with three angles θ_{12}^d, θ_{23}^d, θ_{13}^d and three phases δ_{12}^d, δ_{23}^d, δ_{13}^d, and is obtained with the expression

$$
V_{Hd} = \begin{pmatrix}
c_{12}^d c_{13}^d & s_{12}^d c_{13}^d e^{-i\delta_{12}^d} & s_{13}^d e^{-i\delta_{13}^d} \\
-s_{12}^d c_{23}^d e^{i\delta_{12}^d} - c_{12}^d s_{23}^d s_{13}^d e^{i(\delta_{13}^d - \delta_{23}^d)} & c_{12}^d c_{23}^d - s_{12}^d s_{23}^d s_{13}^d e^{i(\delta_{13}^d - \delta_{12}^d - \delta_{23}^d)} & s_{23}^d c_{13}^d e^{-i\delta_{23}^d} \\
s_{12}^d s_{23}^d e^{i(\delta_{12}^d + \delta_{23}^d)} - c_{12}^d c_{23}^d s_{13}^d e^{i\delta_{13}^d} & -c_{12}^d s_{23}^d e^{i\delta_{23}^d} - s_{12}^d c_{23}^d s_{13}^d e^{i(\delta_{13}^d - \delta_{12}^d)} & c_{23}^d c_{13}^d
\end{pmatrix}. \tag{9}
$$

III. THE CROSS SECTION OF BOTTOM PAIR PRODUCTION IN PHOTON-PHOTON COLLISION

In the LHT model, both T-even and T-odd particles can make the contributions to the process $\gamma\gamma \rightarrow b\bar{b}$. The contributions of T-even particles include both the SM contributions and the contributions of the top quark T-even partner. The contributions of T-odd particles are induced by the interactions between the SM quarks and the mirror quarks mediated by the heavy T-odd gauge bosons or Goldstone bosons. The relevant Feynman diagrams are shown in Fig. 1. In our calculation, we use the dimensional regularization to regulate all the ultraviolet divergences in the virtual loop corrections, and adopt the 't Hooft-Feynman gauge and on-mass-shell renormalization scheme [14]. The renormalized amplitude for $\gamma\gamma \rightarrow b\bar{b}$ contains

$$M_{\mathrm{ren}} = M_0 + \delta M$$
$$= M_0 + \delta M^{\mathrm{self}} + \delta M^{\mathrm{vertex}} + \delta M^{\mathrm{box}} + \delta M^{\mathrm{tr}}, \quad (10)$$

where M_0 is the amplitude at the tree level, δM^{self}, $\delta M^{\mathrm{vertex}}$, δM^{box}, and δM^{tr} represent the contributions arising from the self-energy, vertex, box, and triangle diagrams, respectively. Their explicit forms are given by

$$M_0 = M_0^{\hat{t}} + M_0^{\hat{u}}, \quad (11)$$

$$\delta M^{\mathrm{self}} = \delta M^{s(\hat{t})} + \delta M^{s(\hat{u})}, \quad (12)$$

$$\delta M^{\mathrm{vertex}} = \delta M^{v(\hat{t})} + \delta M^{v(\hat{u})}, \quad (13)$$

$$\delta M^{\mathrm{box}} = \delta M^{b(\hat{t})} + \delta M^{b(\hat{u})}, \quad (14)$$

where

$$M_0^{\hat{t}} = -i\frac{e^2 Q_b^2}{\hat{t} - m_b^2}\epsilon_\mu(p_4)\epsilon_\nu(p_3)\bar{u}(p_2)\gamma^\mu(\not{p}_2 - \not{p}_4 + m_b)$$
$$\times \gamma^\nu v(p_1), \quad (15)$$

$$M_0^{\hat{u}} = M_0^{\hat{t}}(p_3 \leftrightarrow p_4, \hat{t} \leftrightarrow \hat{u}), \quad (16)$$

$$\delta M^{s(\hat{t})} = i\frac{e^2 Q_b^2}{(\hat{t} - m_b^2)^2}\epsilon_\mu(p_4)\epsilon_\nu(p_3)\bar{u}(p_2)$$
$$\times [f_1^{s(\hat{t})}\gamma^\mu\gamma^\nu + f_2^{s(\hat{t})}p_2^\mu\gamma^\nu + f_3^{s(\hat{t})}\not{p}_4\gamma^\mu\gamma^\nu]$$
$$\times v(p_1), \quad (17)$$

$$\delta M^{s(\hat{u})} = \delta M^{s(\hat{t})}(p_3 \leftrightarrow p_4, \hat{t} \leftrightarrow \hat{u}), \quad (18)$$

$$\delta M^{v(\hat{t})} = -i\frac{e^2 Q_b}{\hat{t} - m_b^2}\epsilon_\mu(p_4)\epsilon_\nu(p_3)\bar{u}(p_2)$$
$$\times [f_1^{v(\hat{t})}\gamma^\mu\gamma^\nu + f_2^{v(\hat{t})}\gamma^\mu p_1^\nu + f_3^{v(\hat{t})}p_2^\mu\gamma^\nu$$
$$+ f_4^{v(\hat{t})}p_2^\mu p_1^\nu + f_5^{v(\hat{t})}\not{p}_4\gamma^\mu\gamma^\nu + f_6^{v(\hat{t})}\not{p}_4\gamma^\mu p_1^\nu$$
$$+ f_7^{v(\hat{t})}\not{p}_4 p_2^\mu\gamma^\nu]v(p_1), \quad (19)$$

$$\delta M^{v(\hat{u})} = \delta M^{v(\hat{t})}(p_3 \leftrightarrow p_4, \hat{t} \leftrightarrow \hat{u}), \quad (20)$$

$$\delta M^{b(\hat{t})} = -i\frac{e^2}{16\pi^2}\epsilon_\mu(p_4)\epsilon_\nu(p_3)\bar{u}(p_2)[f_1^{b(\hat{t})}\gamma^\mu\gamma^\nu + f_2^{b(\hat{t})}\gamma^\nu\gamma^\mu + f_3^{b(\hat{t})}\gamma^\mu p_1^\nu + f_4^{b(\hat{t})}p_1^\mu\gamma^\nu + f_5^{b(\hat{t})}\gamma^\mu p_2^\nu + f_6^{b(\hat{t})}p_2^\mu\gamma^\nu$$
$$+ f_7^{b(\hat{t})}p_1^\mu p_1^\nu + f_8^{b(\hat{t})}p_1^\mu p_2^\nu + f_9^{b(\hat{t})}p_2^\mu p_1^\nu + f_{10}^{b(\hat{t})}p_2^\mu p_2^\nu + f_{11}^{b(\hat{t})}\not{p}_4\gamma^\mu\gamma^\nu + f_{12}^{b(\hat{t})}\not{p}_4\gamma^\nu\gamma^\mu + f_{13}^{b(\hat{t})}\not{p}_4\gamma^\mu p_1^\nu$$
$$+ f_{14}^{b(\hat{t})}\not{p}_4 p_1^\mu\gamma^\nu + f_{15}^{b(\hat{t})}\not{p}_4\gamma^\mu p_2^\nu + f_{16}^{b(\hat{t})}\not{p}_4 p_2^\mu\gamma^\nu + f_{17}^{b(\hat{t})}\not{p}_4 p_1^\mu p_1^\nu + f_{18}^{b(\hat{t})}\not{p}_4 p_1^\mu p_2^\nu + f_{19}^{b(\hat{t})}\not{p}_4 p_2^\mu p_1^\nu$$
$$+ f_{20}^{b(\hat{t})}\not{p}_4 p_2^\mu p_2^\nu]v(p_1), \quad (21)$$

$$\delta M^{b(\hat{u})} = \delta M^{b(\hat{t})}(p_3 \leftrightarrow p_4, \hat{t} \leftrightarrow \hat{u}), \quad (22)$$

and

$$\delta M^{\mathrm{tr}} = i\frac{1}{16\pi^2}\epsilon_\mu(p_4)\epsilon_\nu(p_3)\bar{u}(p_2)$$
$$\times [f_1^{\mathrm{tr}}\gamma^\mu\gamma^\nu + f_2^{\mathrm{tr}}\gamma^\nu\gamma^\mu + f_3^{\mathrm{tr}}\gamma^\mu p_1^\nu + f_4^{\mathrm{tr}}p_1^\mu\gamma^\nu$$
$$+ f_5^{\mathrm{tr}}\gamma^\mu p_2^\nu + f_6^{\mathrm{tr}}p_2^\mu\gamma^\nu]v(p_1). \quad (23)$$

Here $\hat{t} = (p_4 - p_2)^2$, $\hat{u} = (p_4 - p_1)^2$, p_3, and p_4 denote the momenta of the two incoming photons, and p_2 and p_1 are the momenta of the outgoing bottom quark and its antiparticle.

The form factors $f_i^{s(\hat{t})}$, $f_i^{v(\hat{t})}$, $f_i^{b(\hat{t})}$, and f_i^{tr} are expressed in terms of two-, three-, and four-point scalar integrals [15], and their analytical expressions are tedious, so we do not present them. We can find that all the ultraviolet divergences cancel in the form factors.

The cross section of the subprocess $\gamma\gamma \rightarrow b\bar{b}$ for the unpolarized photons is given by

$$\hat{\sigma}(\hat{s}) = \frac{N_C}{16\pi\hat{s}^2}\int_{\hat{t}^-}^{\hat{t}^+} d\hat{t}\bar{\sum}_{\mathrm{spins}}|M_{\mathrm{ren}}(\hat{s},\hat{t})|^2, \quad (24)$$

where

$$\hat{t}^\pm = \left(m_b^2 - \frac{1}{2}\hat{s}\right) \pm \frac{1}{2}\hat{s}\sqrt{1 - 4m_b^2/\hat{s}}. \quad (25)$$

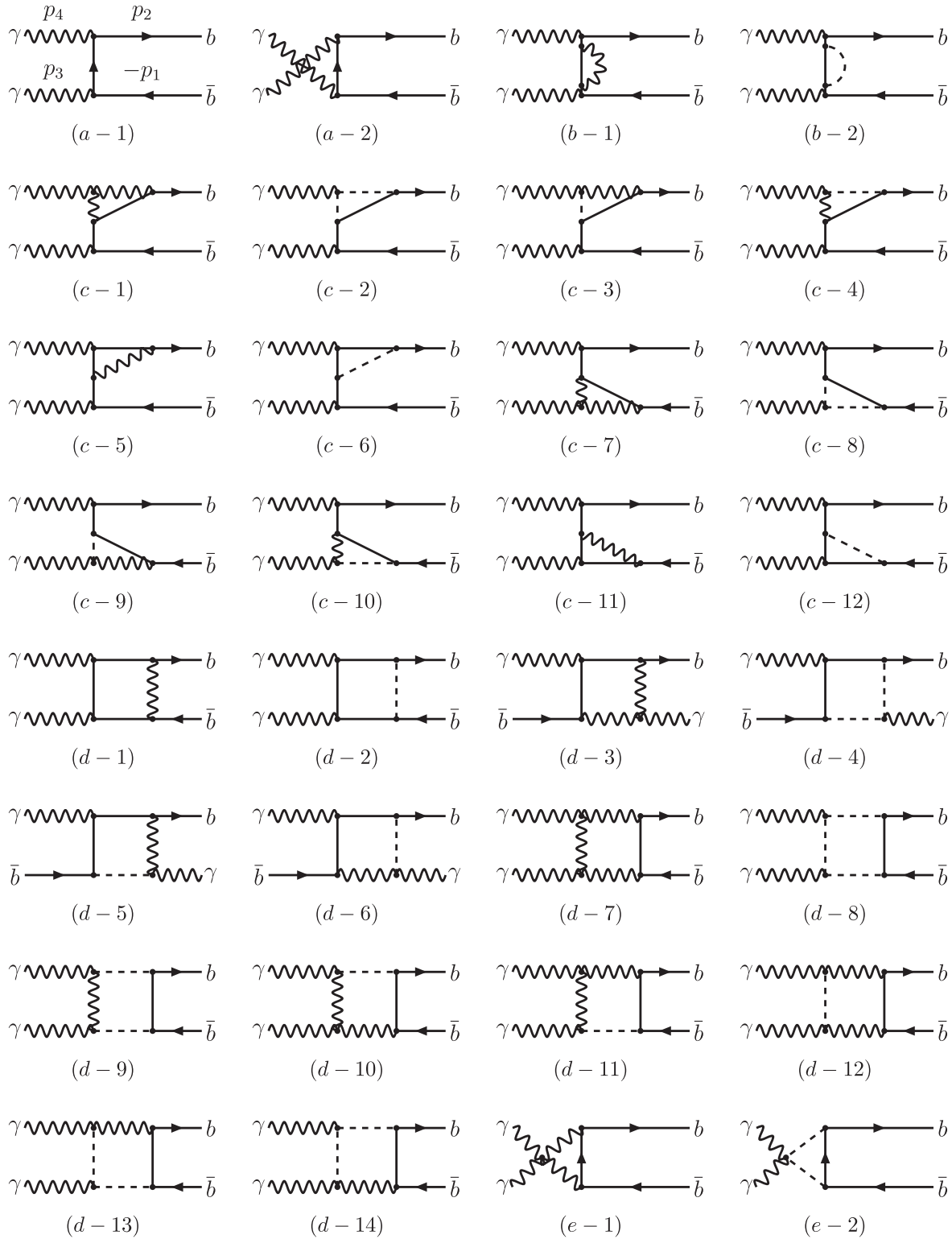The bar over the sum recalls averaging over initial spins and

FIG. 1.   Feynman diagrams for the LHT model contributions to the $\gamma\gamma \rightarrow b\bar{b}$ process: (a) tree-level diagrams; (b) self-energy diagrams; (c) vertex diagrams; (d) box diagrams; (e) triangle diagrams. Here only one-loop diagrams corresponding to the tree-level diagram $(a-1)$ are plotted. The internal wavy lines represent the gauge bosons A_H, Z_H, $W_H^\pm$, and $W_L^\pm$ in the figures $(b-1)$, $(c-5)$, $(c-11)$, and $(d-1)$. The dashed lines indicate the Goldstone bosons ω^0, η, $\omega^\pm$, and $\pi^\pm$ in the figures $(b-2)$, $(c-6)$, $(c-12)$, and $(d-2)$. The internal wavy lines represent the charged gauge bosons $W_H^\pm$ and $W_L^\pm$, together with the dashed lines stand for the charged Goldstone bosons $\omega^\pm$ and $\pi^\pm$ in the figures $(c-1)$–$(c-4)$, $(c-7)$–$(c-10)$, $(d-3)$–$(d-14)$, and $(e-1)$–$(e-2)$. The internal solid lines in all the loops denote the fermions d_H^i, u_H^i, or T_+, which match the corresponding bosons, respectively.

$$\bar{\sum}_{\text{spins}} |M_{\text{ren}}(\hat{s}, \hat{t})|^2 = \bar{\sum}_{\text{spins}} |M_0|^2 + 2 \operatorname{Re} \bar{\sum}_{\text{spins}} M_0^\dagger \delta M. \tag{26}$$

The total cross section $\sigma(s)$ for the bottom pair production can be obtained by folding the elementary cross section $\sigma(\hat{s})$ for the subprocess $\gamma\gamma \to b\bar{b}$ with the photon luminosity at the e^+e^- colliders given in Refs. [4,5], i.e.,

$$\sigma(s) = \int_{2m_b/\sqrt{s}}^{x_{\text{max}}} dz \frac{dL_{\gamma\gamma}}{dz} \hat{\sigma}(\hat{s}), \qquad (\gamma\gamma \to b\bar{b} \text{ at } \hat{s} = z^2 s), \tag{27}$$

where $\sqrt{s}$ and $\sqrt{\hat{s}}$ are the e^+e^- and $\gamma\gamma$ center-of-mass energies, respectively, and $dL_{\gamma\gamma}/dz$ is the photon luminosity, which can be expressed as

$$\frac{dL_{\gamma\gamma}}{dz} = 2z \int_{z^2/x_{\text{max}}}^{x_{\text{max}}} \frac{dx}{x} F_{\gamma/e}(x) F_{\gamma/e}(z^2/x). \tag{28}$$

For unpolarized initial electron and laser beams, the energy spectrum of the backscattered photon is given by [4,16]

$$F_{\gamma/e}(x) = \frac{1}{D(\xi)} \left[1 - x + \frac{1}{1-x} - \frac{4x}{\xi(1-x)} + \frac{4x^2}{\xi^2(1-x^2)} \right], \tag{29}$$

with

$$D(\xi) = \left(1 - \frac{4}{\xi} - \frac{8}{\xi^2} \right) \ln(1 + \xi) + \frac{1}{2} + \frac{8}{\xi} - \frac{1}{2(1+\xi)^2}, \tag{30}$$

where $\xi = 4E_e E_0/m_e^2$ in which m_e and E_e denote, respectively, the incident electron mass and energy, E_0 denotes the initial laser photon energy, and $x = E/E_e$ is the fraction which represents the ratio between the scattered photon and initial electron energy for the backscattered photons moving along the initial electron direction. $F_{\gamma/e}(x)$ vanishes for $x > x_{\text{max}} = E_{\text{max}}/E_e = \xi/(1 + \xi)$. In order to avoid the creation of e^+e^- pairs by the interaction of the incident and backscattered photons, we require $E_0 x_{\text{max}} \leq m_e^2/E_e$ which implies $\xi \leq 2 + 2\sqrt{2} \approx 4.8$ [16]. For the choice $\xi = 4.8$, it can obtain

$$x_{\text{max}} \approx 0.83, \qquad D(\xi) \approx 1.8. \tag{31}$$

IV. NUMERICAL RESULTS AND CONCLUSIONS

There are several free parameters in the LHT model which are involved in the amplitude of $\gamma\gamma \to b\bar{b}$. They are the breaking scale f, the masses of the mirror quarks m_{Hi} ($i = 1, 2, 3$) (here we have ignored the mass difference between up-type mirror quarks and down-type mirror quarks at the order up to $O(v/f)$), the mixing parameter x_L between the SM top quark and its heavy partner T_+ quark, and the other 6 parameters (θ_{12}^d, θ_{13}^d, θ_{23}^d, δ_{12}^d, δ_{13}^d, δ_{23}^d), which are related to the mixing matrix V_{Hd}.

For the parameters f and x_L, some constraints come from the electroweak precision measurements and the Wilkinson microwave anisotropy probe experiment for dark matter relics [17], which shows that the region $f < 570$ GeV is kinematically forbidden. However, these constraints also depend on the other parameters. Hence, we slightly relax the constraints on the parameters f and x_L, and let them vary in the range

$$500 \text{ GeV} \leq f \leq 1500 \text{ GeV}, \qquad 0.1 \leq x_L \leq 0.8, \tag{32}$$

in our numerical calculations.

In Refs. [12,13], the constraints on the mass spectrum of the mirror fermions have been investigated from the analysis of neutral meson mixing in the K, B, and D systems. It has been found that a TeV scale Glashow-Iliopoulos-Maiani suppression is necessary for a generic choice of V_{Hd}. However, there are regions of parameter space which are only very loose constraints on the mass spectrum of the mirror fermions. For the matrix V_{Hd}, we follow Ref. [18] to consider two scenarios for these parameters to simplify our calculations:

(I) $V_{Hd} = 1$. This scenario is connected only with the third-generation mirror quarks due to its involvement in bottom quark and its antiparticle in the final states. Moreover, the constraints on the mass spectrum of the mirror fermions can be relaxed [12]. Therefore, we take

$$500 \text{ GeV} \leq m_{H3} \leq 3000 \text{ GeV}, \tag{33}$$

to see its effect.

(II) $s_{23}^d = 1/\sqrt{2}$, $s_{12}^d = s_{13}^d = 0$, $\delta_{12}^d = \delta_{23}^d = \delta_{13}^d = 0$. In this scenario, the D meson system can give strong constraints on the relevant parameters [12]. Considering these constraints, we fix $m_{H_1} = m_{H_2} = 500$ GeV, and take the same assumption as in Scenario I for the third-generation mirror quarks.

In our numerical evaluation, we take a set of independent input parameters which are known from current experiment. The input parameters are $m_t = 171.2$ GeV, $m_b = 4.2$ GeV, $M_W = 80.398$ GeV, $M_Z = 91.1876$ GeV, $\alpha = 1/137.036$, and $G_F = 1.166\,37 \times 10^{-5}$ GeV^{-2} [19]. For the c.m. energies of the International Linear Collider (ILC), we choose $\sqrt{s} = 500, 1000$ GeV according to the ILC Reference Design Report [20]. The final numerical results are summarized in Figs. 2–4.

Figure 2 shows the total cross section $\sigma(e^+e^- \to \gamma\gamma \to b\bar{b})$ versus f with $\sqrt{s} = 500$ GeV and $x_L = 0.3$, in which the dashed lines, dotted lines, and dot-dashed lines denote the cases of $m_{H3} = 500, 1000, 1500$ GeV, respectively, and the solid lines stand for the results of the tree level. From this figure, we can obtain the following results: (i) The cross section is strongly dependent on the parameter f, and is about a few percent to dozens of percent larger than that of the tree level. It is natural since the couplings between
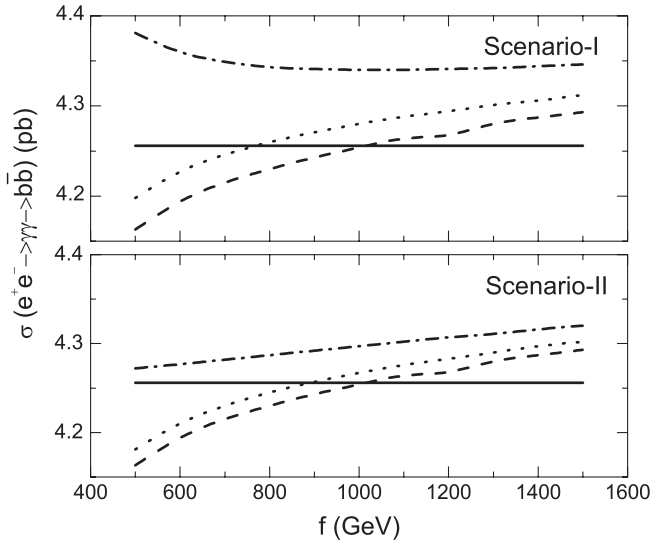
FIG. 2. The total cross section $\sigma(e^+e^- \to \gamma\gamma \to b\bar{b})$ as a function of f for $\sqrt{s} = 500$ GeV and $x_L = 0.3$. The dashed lines, dotted lines, and dot-dashed lines denote, respectively, the cases of $m_{H3} = 500$, 1000, 1500 GeV, and the solid lines stand for the results of the tree level.
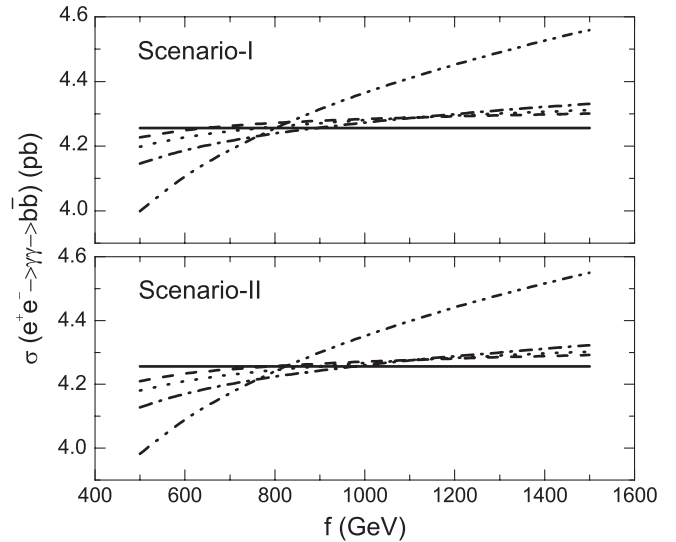

FIG. 3. The total cross section $\sigma(e^+e^- \to \gamma\gamma \to b\bar{b})$ versus f with $\sqrt{s} = 500$ GeV and $m_{H3} = 1000$ GeV. The dashed lines, dotted lines, dot-dashed lines, and dot-dot-dashed lines indicate the cases of $x_L = 0.1$, 0.3, 0.5 and 0.8, respectively, and the solid lines represent the results of the tree level.

the new top quark T_+ and the SM quarks are proportional to the mass of T_+ quark; i.e., are proportional to the breaking scale f. Furthermore, our analytical calculations also show that the contributions from the heavy T-odd gauge bosons and Goldstone bosons increase slightly with f for $m_{H3} \leq 1000$ GeV, and decrease slowly when $m_{H3} > 1000$ GeV; (ii) Since the couplings between the mirror quarks and the SM quarks are proportional to the mirror quark masses, the cross section increases distinctly with f for the cases of m_{H3} from 500, 1000 to 1500 GeV, while the relative section cross is negative when all of f and m_{H3} take small values; and (iii) Comparing these two scenarios, we can see that the cross section for Scenario II does not have a large deviation from that for Scenario I when m_{H3} takes a small value, but the former is only about a half of the latter for a large value of m_{H3}.

The cross section $\sigma(e^+e^- \to \gamma\gamma \to b\bar{b})$ versus the parameter f for various values x_L when $\sqrt{s} = 500$ GeV and $m_{H3} = 1000$ GeV is given in Fig. 3. We can see that: (i) the correction of the LHT model to the cross section changes from negative to positive with f becoming large; (ii) the increment of the cross section with f is slow for the cases of $x_L = 0.1$, 0.3, 0.5 and is quick for $x_L = 0.8$; and (iii) the behavior of the cross section for Scenario II is almost the same as that for Scenario I.

For the case of $\sqrt{s} = 1000$ GeV, our calculations show that the effect of the LHT model in this case is slightly larger than that in the case of $\sqrt{s} = 500$ GeV.

In order to look at the relative correction of the LHT model to the cross section, we take $f = 700$ GeV and $x_L = 0.3$ as an example and plot $\delta\sigma(e^+e^- \to \gamma\gamma \to b\bar{b})$ as a function of m_{H3} in Fig. 4. From this figure, we can find

that (i) the contribution of the LHT model to the process is very obvious unless m_{H3} is small; (ii) for the case of $\sqrt{s} = 500$ GeV, the relative correction, $\delta\sigma(e^+e^- \to \gamma\gamma \to b\bar{b})$, is sensitive to m_{H3}, and increases with m_{H3} from -0.97% to 25.71% for Scenario I and from -0.97% to 12.37% for Scenario II; and (iii) for $\sqrt{s} = 1000$ GeV, the relative correction changes from $-0.99\% \sim 26.32\%$ for Scenario I, and $-0.99\% \sim 12.66\%$ for Scenario II.

We know that the ILC is the important next generation linear collider. According to the ILC Reference Design
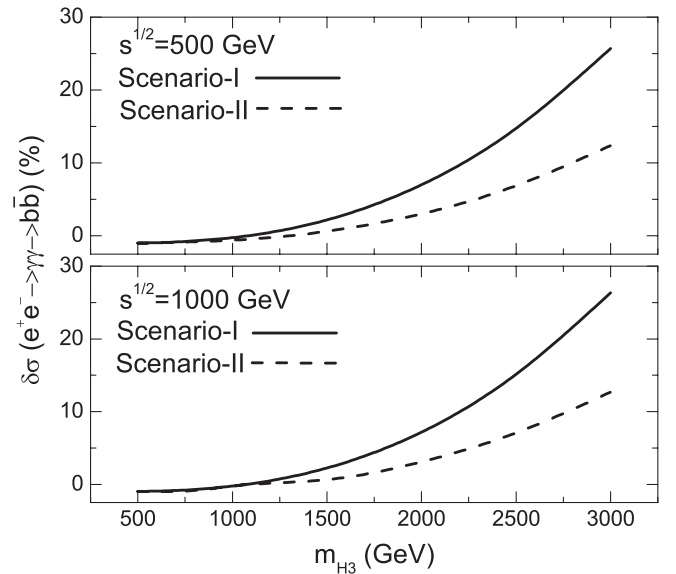

FIG. 4. The relative correction of the LHT model to the cross section, $\delta\sigma(e^+e^- \to \gamma\gamma \to b\bar{b})$, as a function of m_{H3} with $f = 700$ GeV and $x_L = 0.3$.

Report [20], the ILC is determined to run with $\sqrt{s} = 500$ GeV (upgradeable to 1000 GeV) and the total luminosity required is $L = 500$ fb^{-1} with the first four-year operation and $L = 1000$ fb^{-1} during the first phase of operation with $\sqrt{s} = 500$ GeV. It means that millions of the bottom pairs per year can be produced, and the relative correction of the LHT model to the cross section can reach the level from a few percent to dozens of percent when m_{H3} takes a larger value. However, the relative correction induced by the charged Higgs and charged Goldstone bosons in the 2HDM and MSSM is less than 0.1% [5], and in the TC2 model, the relative correction from the pseudo-Goldstone bosons and the new gauge bosons is negative and no more than 10% [6]. Furthermore, our calculations show that the contribution of Higgs boson in the SM is only the order of 10^{-6} which is negligibly small. Therefore via the process $e^+e^- \rightarrow \gamma\gamma \rightarrow b\bar{b}$, the LHT model is experimentally distinguishable from the SM, 2HDM, MSSM, and TC2 models, which affords the possibility to test the LHT model at the ILC unless u_H^3 and d_H^3 are very light. It is hoped that ILC will be able to give strong constraints on the relevant parameters of LHT model since the correction of the LHT model to the cross section of $e^+e^- \rightarrow \gamma\gamma \rightarrow b\bar{b}$ is sensitive to some parameters.

In conclusion, we have studied the contribution of the LHT model to the process $e^+e^- \rightarrow \gamma\gamma \rightarrow b\bar{b}$. We find that, for the favorable parameters, the total cross section $\sigma(e^+e^- \rightarrow \gamma\gamma \rightarrow b\bar{b})$ is sensitive to the breaking scale f, the mixing parameter x_L, the masses of the mirror quarks m_{Hi}, and the relative correction of the LHT model is a few percent to dozens of percent unless m_{H3} is very small. The total cross section is significantly larger than the corresponding results in the standard model, the general two Higgs doublet model, the minimal supersymmetric standard model, and the topcolor assisted technicolor model. Therefore the difference is obvious for the International Linear Colliders and it is really interesting in testing the standard model and searching for the signs of the littlest Higgs model with T parity.

ACKNOWLEDGMENTS

[1] S. J. Brodsky and P. M. Zerwas, Nucl. Instrum. Methods Phys. Res., Sect. A **355**, 19 (1995).

[2] I. F. Ginzburg, G. L. Kotkin, V. G. Serbo, and V. I. Telnov, Pis'ma Zh. Eksp. Teor. Fiz. **34**, 514 (1981); Nucl. Instrum. Methods Phys. Res. **205**, 47 (1983).

[3] F. Halzen, C. S. Kim, and M. L. Stong, Phys. Lett. B **274**, 489 (1992).

[4] O. J. P. Eboli, M. C. Gonzalez-Garcia, F. Halzen, and S. F. Novaes, Phys. Rev. D **47**, 1889 (1993).

[5] L. Han, C. G. Hu, C. S. Li, and W. G. Ma, Phys. Rev. D **54**, 2363 (1996).

[6] J. S. Huang and G. R. Lu, Phys. Rev. D **78**, 035007 (2008).

[7] N. Arkani-Hamed, A. G. Cohen, and H. Georgi, Phys. Lett. B **513**, 232 (2001); N. Arkani-Hamed *et al.*, J. High Energy Phys. 08 (2002) 020; 08 (2002) 021; I. Low, W. Skiba, and D. Smith, Phys. Rev. D **66**, 072001 (2002); D. E. Kaplan and M. Schmaltz, J. High Energy Phys. 10 (2003) 039.

[8] N. Arkani-Hamed, A. G. Cohen, E. Katz, and A. E. Nelson, J. High Energy Phys. 07 (2002) 034; S. Chang, J. High Energy Phys. 12 (2003) 057; T. Han, H. E. Logan, B. McElrath, and L. T. Wang, Phys. Rev. D **67**, 095004 (2003); M. Schmaltz and D. Tucker-Smith, Annu. Rev. Nucl. Part. Sci. **55**, 229 (2005); A. J. Buras, A. Poschenrieder, and S. Uhlig, Nucl. Phys. **B716**, 173 (2005); A. J. Buras, A. Poschenrieder, S. Uhlig, and W. A. Bardeen, J. High Energy Phys. 11 (2006) 062.

[9] C. Csaki, J. Hubisz, G. D. Kribs, P. Meade, and J. Terning, Phys. Rev. D **67**, 115002 (2003); **68**, 035009 (2003); J. L. Hewett, F. J. Petriello, and T. G. Rizzo, J. High Energy Phys. 10 (2003) 062; M. C. Chen and S. Dawson, Phys. Rev. D **70**, 015003 (2004); M. C. Chen *et al.*, Mod. Phys. Lett. A **21**, 621 (2006); W. Kilian and J. Reuter, Phys. Rev. D **70**, 015004 (2004).

[10] G. Marandella, C. Schappacher, and A. Strumia, Phys. Rev. D **72**, 035014 (2005).

[11] H. C. Cheng and I. Low, J. High Energy Phys. 09 (2003) 051; 08 (2004) 061; I. Low, J. High Energy Phys. 10 (2004) 067; J. Hubisz and P. Meade, Phys. Rev. D **71**, 035016 (2005).

[12] J. Hubisz, S. J. Lee, and G. Paz, J. High Energy Phys. 06 (2006) 041.

[13] M. Blanke *et al.*, J. High Energy Phys. 12 (2006) 003; 01 (2007) 066; X. F. Han, L. Wang, and J. M. Yang, Phys. Rev. D **78**, 075017 (2008); Qing-Hong Cao, Chuan-Ren Chen, F. Larios, and C.-P. Yuan, Phys. Rev. D **79**, 015004 (2009).

[14] M. Bohm, H. Spiesberger, and W. Hollik, Fortschr. Phys. **34**, 687 (1986); W. Hollik, *ibid.* **38**, 165 (1990); B. Grzadkowski and W. Hollik, Nucl. Phys. **B384**, 101 (1992).

[15] M. Clements, C. Footman, A. Kronfeld, S. Narasimhan, and D. Photiadis, Phys. Rev. D **27**, 570 (1983); A. Axelrod, Nucl. Phys. **B209**, 349 (1982); G. Passarino and M. Veltman, *ibid.* **B160**, 151 (1979).

[16] K. M. Cheung, Phys. Rev. D **47**, 3750 (1993); H. Y. Zhou *et al.*, *ibid.* **57**, 4205 (1998); B. Zhang, Y. N. Gao, and Y. P. Kuang, *ibid.* **70**, 115012 (2004); I. Sahin, Eur. Phys. J. C **60**, 431 (2009).

[17] J. Hubisz, P. Meade, A. Noble, and M. Perelstein, J. High Energy Phys. 01 (2006) 135; S. Matsumoto, T. Moroi, and K. Tobe, Phys. Rev. D **78**, 055018 (2008).

[18] H.-S. Hou, Phys. Rev. D **75**, 094010 (2007); X. F. Han, L. Wang, and J. M. Yang, arXiv:0903.5491.

[19] C. Amsler *et al.*, Phys. Lett. B **667**, 1 (2008).

[20] J. Brau, Y. Okada, and N. Walker, arXiv:0712.1950; A. Djouadi *et al.*, arXiv:0709.1893; N. Phinney, N. Toge, and N. Walker, arXiv:0712.2361; T. Behnke, C. Damerell, J. Jaros, and A. Myamoto, arXiv:0712.2356.